International Journal of Mass Spectrometry 429 (2018) 90–100

Contents lists available at ScienceDirect

International Journal of Mass Spectrometry

journal homepage: www.elsevier.com/locate/ijms

Dehydration reactions of protonated dipeptides containing asparagine or glutamine investigated by infrared ion spectroscopy

Lisanne J.M. Kempkes[a], Jonathan Martens[a], Giel Berden[a], Jos Oomens[a,b,*]

[a] Radboud University, Institute for Molecules and Materials, FELIX laboratory, Toernooiveld 7c, 6525 ED Nijmegen, The Netherlands
[b] Van't Hoff Institute for Molecular Sciences, University of Amsterdam,Science Park 904, 1098 XH Amsterdam, The Netherlands

ARTICLE INFO

Article history:
Received 22 February 2017
Received in revised form 12 May 2017
Accepted 7 June 2017
Available online 17 June 2017

Dedicated On the occasion of the 70th birthday of our friend and mentor Terrance B. McMahon.

Keywords:
Peptide fragmentation mechanisms
IRMPD spectroscopy
H_2O-loss
Glutamine
Asparagine

ABSTRACT

The role of specific amino acid side-chains in the fragmentation chemistry of gaseous protonated peptides resulting from collisional activation remains incompletely understood. For small peptides containing asparagine and glutamine, a dominant fragmentation channel induced by collisional activations is, in addition to deamidation, the loss of neutral water. Identifying the product ion structures from H_2O-loss from four protonated dipeptides containing Asn or Gln using infrared ion spectroscopy, mechanistic details of the dissociation reactions are revealed. Several sequential dissociation reactions have also been investigated and provide additional insights into the fragmentation chemistry. While water loss can in principle occur from the C-terminus, the side chain or the amide bond carbonyl oxygen, in most cases the C-terminus was found to detach H_2O, leading to a b_2-sequence ion with an oxazolone structure for AlaGln, and bifurcating mechanisms leading to both oxazolone and diketopiperazine species for AlaAsn and AsnAla. In contrast, GlnAla expels water from the amide side chain leading to an imino-substituted prolinyl structure.

1. Introduction

Tandem mass spectrometry has become an indispensable tool in proteomics as it enables the routine determination of the amino acid sequence of peptides and proteins. This process involves the gas-phase dissociation of the protonated peptide and an analysis of the *m*/*z* values of the resulting fragment ions. In its most common form, dissociation is accomplished through collisional activation. Collision-induced dissociation (CID) primarily leads to backbone dissociation at the amide bonds, generating sequence ions referred to as b-type (N-terminal) or y-type (C-terminal) [1–8]. The molecular structures of the resulting b-type ions have been under particularly vigorous debate and it has now been established that b-type ions most often possess an oxazolone structure; for b_2-fragment ions, a diketopiperazine structure is in some cases formed alternatively [9]. Collision-induced migration of a proton from the most basic site to the amide bond where dissociation occurs, accompanied by a nucleophilic attack by the adjacent backbone carbonyl oxygen or the N-terminal nitrogen are suggested as the reaction pathways to these product ion structures, respectively [10–12]. Deviations from this general behavior have also been observed, for instance, b-ions from GlyGlyGly contain both five- and eight-membered ring structures [13]. Furthermore, the side chain can become actively involved in the reaction mechanism for instance in the formation of b_2 ions from protonated PheGlnAla (a glutarimide structure) and AlaAsnAla (a succinimide structure) [3].

Small molecule loss upon CID often occurs in addition to backbone fragmentation, where ammonia (deamidation) and water (dehydration) loss are the most common examples. The resulting non-sequence ions are typically not used for protein identification as their *m*/*z* values are often not recognized by sequencing algorithms [11,14,15]. However, since these processes are so common, a mechanistic understanding is of importance and may aid in further improving the interpretation of CID MS/MS spectra and the accuracy of sequencing [1].

In a recent publication [16], we investigated the deamidation of four very similar dipeptides in order to compare the influence of the side chain identity – Asparagine (Asn) versus Glutamine (Gln) – and the amino acid sequence – AlaXxx versus XxxAla, where Xxx is Asn or Gln. Here, we complement these studies by an investigation of the elimination of water from these same four peptides, so that we are able to completely map out their dissociation chemistry. Structures of the product ions were determined using a combina-

* Corresponding author at: Radboud University, Institute for Molecules and Materials, FELIX laboratory, Toernooiveld 7c, 6525 ED Nijmegen, The Netherlands.
E-mail address: joso@science.ru.nl (J. Oomens).

https://doi.org/10.1016/j.ijms.2017.06.004
1387-3806/

tion of mass spectrometry, infrared multiple photon dissociation (IRMPD) spectroscopy and theoretical calculations. IRMPD spectroscopy has previously been used to determine the structures of several protonated peptide precursor ions and fragments [17–22], and has proven to be a powerful method to distinguish isomers, (prototropic) tautomers and conformers [18,21,23–33].

Various studies have examined the product structures of water loss from different protonated peptides [34–36], considering in particular the influence of the side chain [2,3,9], peptide length and the identity of the terminal residue in the departing fragment [9]. Note that water loss from an *n*-residue peptide gives a product ion corresponding to the b_n sequence ion (at least in terms of its *m*/*z* value). Water loss from ArgGly and AsnGly has been shown to lead to an oxazolone b_2 fragment, while for GlyArg it leads to a diketopiperazine structure [37,38]. The b_2 ions of HisAla bifurcate to both oxazolone and diketopiperazine fragment ions [9,39]. However, for protonated GlyGlyGlyGly, water loss occurs from the N-terminal amide group, initiated by a nucleophilic attack of the neighboring amide nitrogen, and hence does not result in an oxazolone structure [40]. While, GlyGly dissociation does not form a b-ion, b-ions from GlyGlyGly contain both five- and eight-membered ring structures [13]. Tripeptides that contain Asn or Gln have been shown to dissociate along different fragmentation mechanisms [2,3,9].

In order to understand why the formation of b_2-ions from AsnAlaAla and AlaAsnAla follow different reaction mechanisms, we have selected simplified dipeptide systems. These insights are valuable for understanding the fragmentation behavior of small peptides, and can be extrapolated to explain the fragmentation mechanisms of larger peptides and proteins and can as well be used to predict which reaction mechanisms lead to the formation of b_2 ions and which lead to the loss of small neutrals.

For the four dipeptides investigated here, Alanine-Asparagine (AlaAsn), Asparagine-Alanine (AsnAla), Alanine-Glutamine (AlaGln) and Glutamine-Alanine (GlnAla), loss of neutral ammonia and water are the dominant reaction channels upon collisional activation. The dehydration reaction of these dipeptides can lead to b_2-type ions if loss of water occurs from the C-terminus, however, water loss can potentially also occur from the peptide bond carbonyl or from the side-chain. Dehydration via the amide side chain can take place following a reaction that is similar to the reaction mechanism for the loss of ammonia [16]. To support the identification of the dehydrated ion structures, secondary fragmentation reactions were also studied providing further confirmation for the identified structures and allowing us to construct a comprehensive map of the reaction network for each of the peptides is presented.

2. Experimental and computational methods

2.1. IRMPD spectroscopy

To obtain infrared multiple-photon dissociation (IRMPD) spectra of the dehydrated peptide fragment ions, a modified 3D quadrupole ion trap mass spectrometer (Bruker, AmaZon Speed ETD) was used [41,42] in combination with the Free Electron Laser for Infrared eXperiments (FELIX) [43]. IRMPD spectra were recorded over the 800–2000 cm^{-1} region. For IRMPD spectra in the hydrogen stretching range (3200–3800 cm^{-1}), an optical parametric oscillator (OPO, Laser Vision, Bellevue, USA) was used [44]. Employing FELIX, ions were irradiated with 6 μs long macropulses at a repetition rate of 10 Hz, each pulse having an energy of approximately 40 mJ and a bandwidth of ~0.5% of the center frequency. The Nd:YAG-pumped OPO generates 5 ns long pulses of approximately 15 mJ at 10 Hz and has a bandwidth of approximately 3 cm^{-1}. The frequency of FELIX is calibrated using a grating spectrometer and a wavemeter is used for the OPO. IRMPD spectra are corrected for fluctuations of the pulse energy over the scan range assuming a linear power dependence of the fragmentation signal.

Protonated peptide ions were generated using electrospray ionization (ESI) from 10^{-6} M solutions in 50:50 acetonitrile:water with ~0.1% formic acid added. Collisional activation of the isolated dipeptides for 40 ms with an amplitude parameter of approximately 0.3 V generated the $[M+H-H_2O]^+$ ions, which were subsequently mass selected and irradiated with two (more for OPO measurements) pulses from the IR laser. The IR induced fragment yield at each wavelength is obtained from five averaged mass spectra and calculated by relating the parent and fragment ion intensities according to $\sum I(fragments)/\sum I(fragments + parent)$ [42,45]. Peptides were purchased from GeneCust (Luxembourg) and used without any further purification.

2.2. Computational chemistry

Density Functional Theory (DFT) calculations were performed at the B3LYP/6-31++G(d,p) level of theory using Gaussian 09 revision D01 [46]. Molecular geometries of the peptide fragment ions were optimized for different conceivable protonation sites and their linear IR spectra were predicted. Computed harmonic vibrational frequencies were scaled by 0.975 and convoluted with a 25 cm^{-1} full-width-at-half-maximum (FWHM) Gaussian line shape to facilitate comparison with experimental spectra. In order to obtain the lowest energy conformers and to explore the potential energy surface, a molecular mechanics/molecular dynamics (MM/MD) approach using AMBER 12 [16,41,44,47] was applied on each peptide fragment ion. MS^3 fragments were considered to be small enough that no MM/MD approach was required. After an initial MM geometry optimization within AMBER, a simulated annealing procedure up to 500 K was used to obtain 500 structures. These structures were grouped based on their structural similarity using appropriate rms criteria to give 20–30 candidate structures. These structures were then optimized using the DFT protocol and their scaled harmonic spectra were compared with the experimental spectra. The computational procedure is described in more detail elsewhere [25,41,44].

3. Results

3.1. Dehydrated alanine-asparagine, $[AlaAsn+H-H_2O]^+$

As depicted in Scheme 1, several possible mechanisms leading to the expulsion of H_2O were considered. Table 1 presents the three lowest energy structures arising from these calculations. Additional structures with their relative energies can be found in Table S1 of the Supplementary information. The colors of the molecules in the tables correspond to the colors of the arrows indicating the nucleophilic attacks in Scheme 1. For each of the resulting structures, multiple protonation sites are conceivable as indicated by numbers 1–6 in the first column of Table 1. Structure **1.5**, the oxygen-protonated diketopiperazine structure, is the overall lowest energy structure.

For $[AlaAsn+H-H_2O]^+$, two distinct fragments are produced by IRMPD, one at *m*/*z* 169 (corresponding to loss of NH_3, top left panel in Fig. 1) and the other at *m*/*z* 158 (loss of CO, bottom left panel). The latter is accompanied by a minor dissociation into *m*/*z* 141 corresponding to additional NH_3 loss. Determining the IRMPD yield separately for these two channels gives two distinct IRMPD spectra, suggesting that multiple isomers are present in the population of $[AlaAsn+H-H_2O]^+$, each following distinct fragmentation pathways.

The band near 1925 cm^{-1} in the spectrum encoded into the CO and $CO+NH_3$ loss channels (Fig. 1, bottom left) is the characteristic

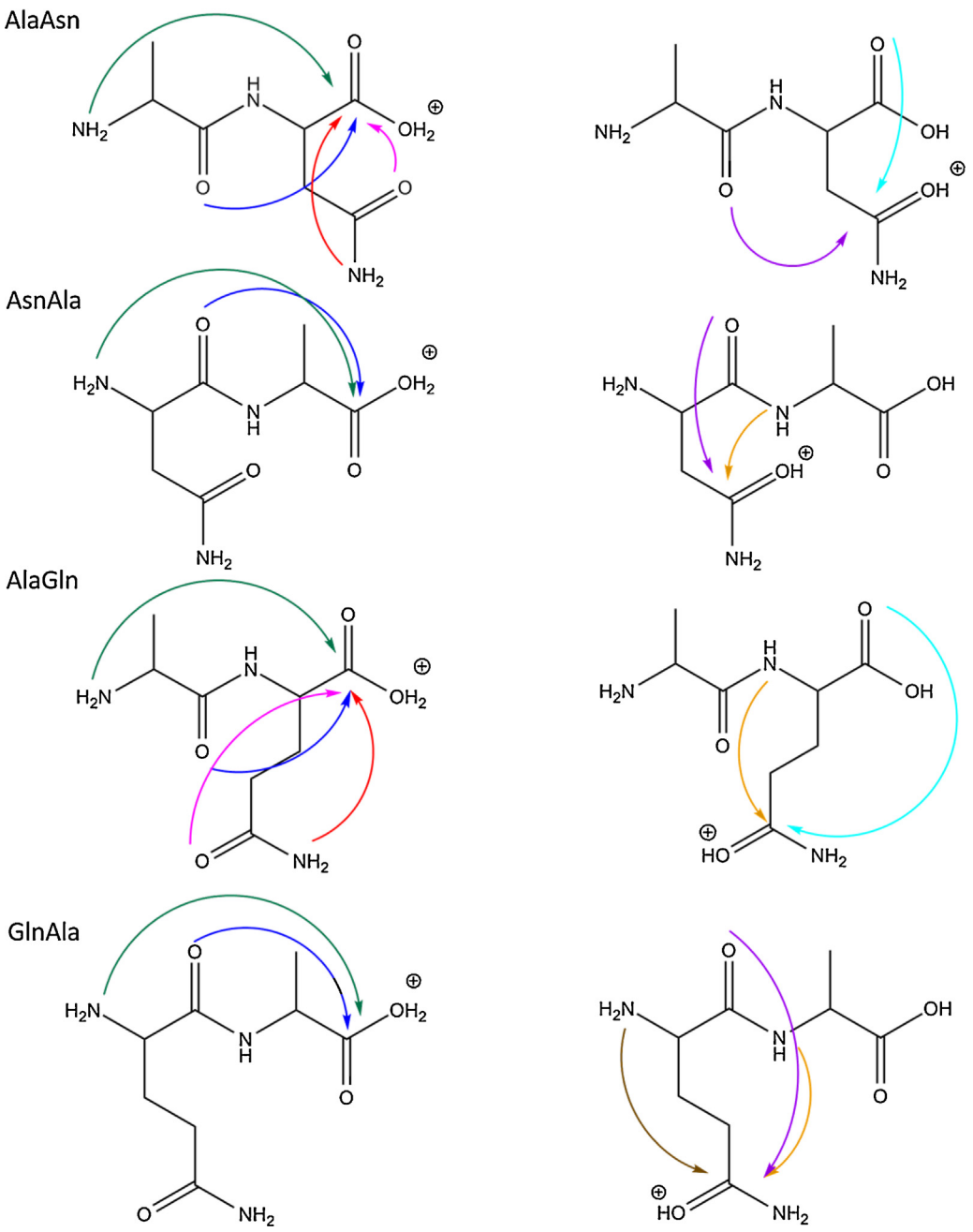

Scheme 1. Possible nucleophilic attack rearrangements leading to dehydration. Both the attack on the C-terminus (left column) as well as on the side chain (right column) are considered. Mechanisms leading to energetically less favorable 4–,7- or higher membered ring structures are not shown here as they were consistently found to lead to high-energy fragment structures. Analogous reaction mechanisms are indicated by arrows of the same color.

C=O stretch of an oxazolone ring thus identifying the oxazolone structure **2**. In fact, this band shows a splitting which suggests that the two lowest-energy oxazolone tautomers co-exist and the spectrum between 1000 and 1800 cm^{-1} agrees with the calculated IR spectra of both **2.3** and **2.5**. The relative Gibbs free energy difference between them is only 9 kJ/mol, which makes transfer of the proton from the oxazolone ring to the N-terminus thermodynamically possible as has been previously observed [9,18]. The band at 1710 cm^{-1} is assigned to C=O stretching of the side chain amide and the band around 1600 cm^{-1} is assigned to NH_2 bending at the N-terminus.

In contrast, the absence of the oxazolone band in the spectrum around 1900 cm^{-1} encoded into the NH_3-loss channel is a strong indication that the carrier has a diketopiperazine structure (**1**). The small peaks in the 1800–2000 cm^{-1} range are likely due to minor NH_3 loss from the oxazolone structure. Protonation on each of the distinguishable diketopiperazine oxygens leads to different H-bond stabilized structures (**1.5** and **1.6**) and comparison with their computed spectra in green and grey suggests the presence of more than one tautomer is evident [9]. The band around 1760 cm^{-1} in the calculated spectra of both tautomers is due to the unprotonated carbonyl C=O stretch. The band near 1420 cm^{-1} is due to CH bending in the CH_3-group. Several weaker bands predicted in the 1000-1400 cm^{-1} range are barely visible in the experimental spectrum. The intense band predicted at 1180 cm^{-1} is not observed in the experiment; the computation shows that it is due to a normal mode with dominant $O-H^+\cdots O$ bending character, which we suspect to be subject to significant spectral broadening and shifting in

Table 1
Calculated relative Gibbs free energies in kJ/mol for the different possible isomeric structures resulting from H_2O loss from protonated AlaAsn, each given for different conceivable protonation sites. The colors of the structures correspond with the colors of the arrows in Scheme 1.

Name → ↓ $[H]^+$ Site	**1 Diketopiperazine**	**2 Oxazolone**	**4 Succinimide**
1	[a]	+ 185	+ 186
2	+ 59	+ 157	+ 35
3	+ 66	+ 50	+ 20
4	+ 103	+ 143	
5	**0**	+ 59	
6	+ 29		

[a] Proton migrates to position 5 during optimization.

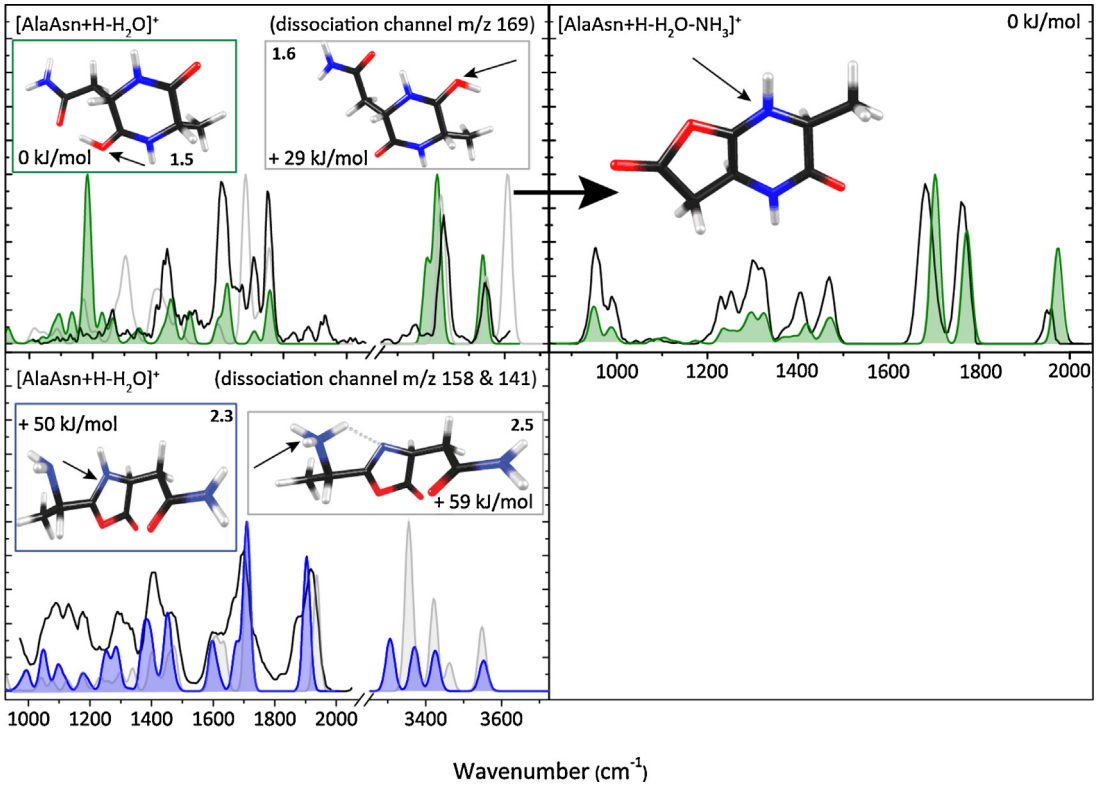

Fig. 1. IRMPD spectra (black) of $[AlaAsn+H-H_2O]^+$ (left panels) and $[AlaAsn+H-H_2O-NH_3]^+$ (right panel) compared to calculated spectra. The IRMPD spectra of $[AlaAsn+H-H_2O]^+$ in the left panels are generated by plotting the wavelength-dependent fragmentation into the *m/z* 169 channel (top, loss of NH_3) and that into the *m/z* 158 and 141 channels summed (bottom, loss of CO and $CO+NH_3$). Experimental spectra are plotted along with the best matching theoretical spectrum, where colors correspond to Table 1. The spectrum of the $[AlaAsn+H-H_2O-NH_3]^+$ MS^3 fragment ion (top right) confirms its structure as being formed from the diketopiperazine. Protonation sites are indicated with arrows.

the IRMPD spectrum and to poor modelling by the harmonic calculations [48–53]. Other isomers/tautomers have been considered, but no convincing spectral match was found (see Fig. S1 in the Supporting information) and these structures are not further discussed here.

The right panel of Fig. 1 shows the IRMPD spectrum of the MS^3 fragment $[AlaAsn+H-H_2O-NH_3]^+$ at *m/z* 169. Based on the agreement of the experimental spectrum with the predicted spectrum for a structure arising from NH_3 loss from the amide side chain of **1**, we assign the structure of this secondary fragment as a lactone/diketopiperazine fused ring structure. The band around 1975 cm^{-1} is due to carbonyl C=O stretching in the lactone ring, the 1775 cm^{-1} band is assigned to C=O stretching in the diketopiperazine ring, and the band near 1710 cm^{-1} is CN stretching of the protonated nitrogen. This assignment lends further support to the identification of $[AlaAsn+H-H_2O]^+$ as **1**. The intensity of the $[AlaAsn+H-H_2O-CO]^+$ product was too low to investigate its structure by IRMPD spectroscopy.

Scheme 2a shows the bifurcating reaction mechanism in the dehydration of protonated AlaAsn suggested by the present spectroscopic observations. Both isomers are formed through H_2O-loss from the C-terminus. To form the diketopiperazine isomer, nucleophilic attack occurs from the N-terminus, while the oxazolone isomer is formed via nucleophilic attack from the peptide bond oxygen. These pathways thus follow the well-known *b-y* fragmentation mechanism for protonated peptides [8]. Subsequent MS^3 dissociation of the diketopiperazine expels NH_3 from the Asn side chain. The oxazolone isomer expels CO, probably leading to an *a*-type

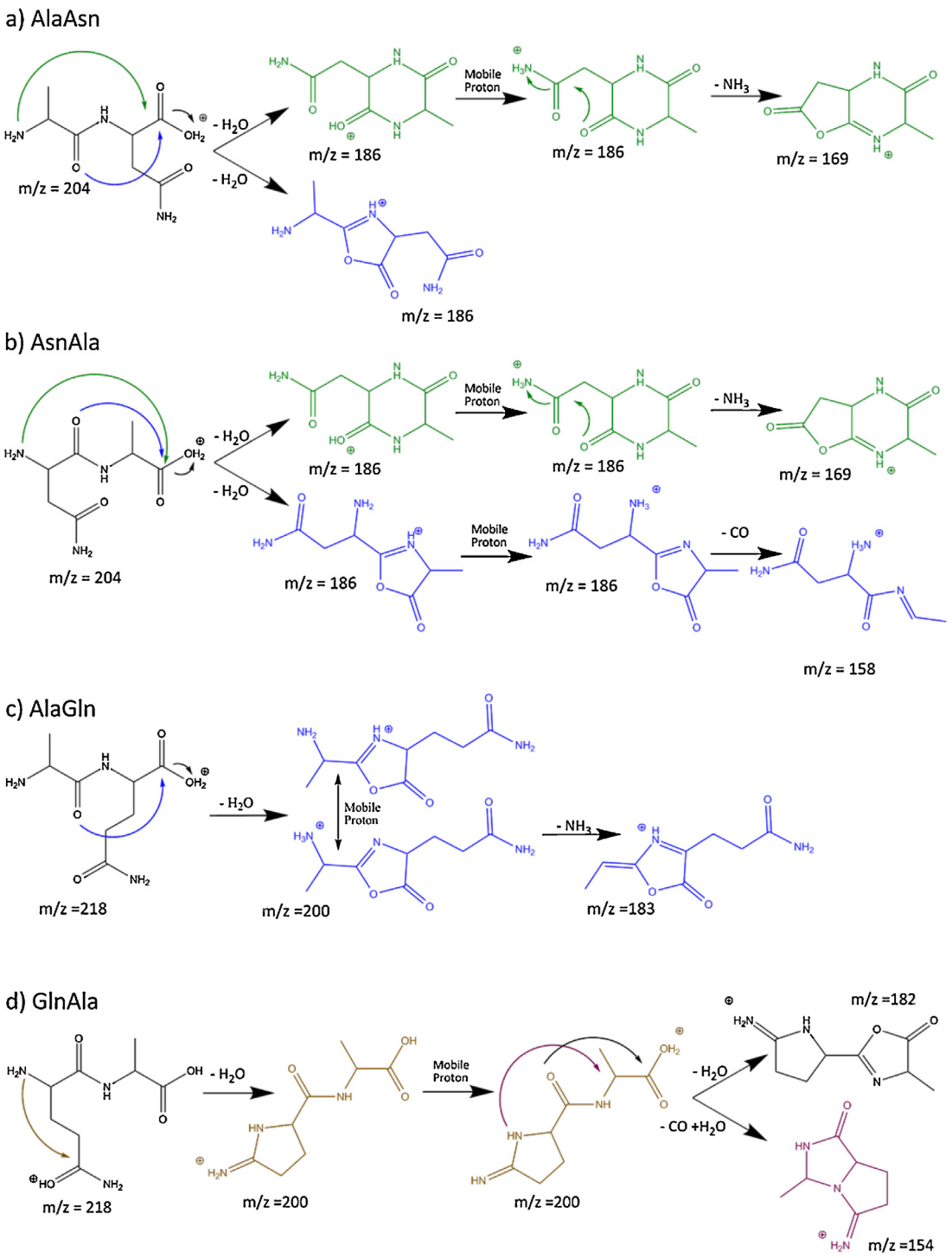

Scheme 2. Proposed reaction mechanisms for H_2O-loss from the dipeptides investigated as derived from the product ion structures identified based on their IRMPD spectra.

sequence ion, although no spectroscopic information is available here (see further in the discussion of AsnAla).

Assuming that the diketopiperazine structure dissociates exclusively via NH_3 loss (into *m/z* 169) and that the oxazolone dissociates exclusively via loss of CO and CO+NH_3 (into *m/z* 158 and 141), we can use the CID MS^3 spectrum to estimate the relative dissociation rates into the bifurcating oxazolone and diketopiperazine pathways upon dehydration of the precursor peptide $[AlaAsn+H]^+$. Fig. S5 in the Supporting information shows that this ratio is about 4.5–1 in favor of the diketopiperazine pathway.

3.2. Dehydrated asparagine-alanine, $[AsnAla+H- H_2O]^+$

For $[AsnAla+H-H_2O]^+$, Scheme 1 presents four possible reaction mechanisms leading to isomers **6–9**, for each of which all potential protonation sites have been considered; computed relative Gibbs free energies are shown in Table 2 for the most prominent ones, with additional structures given in Table S2 in the SI. Ions **6** and **7** arise from H_2O loss from the C-terminus, while **8** and **9** form upon H_2O loss from the side chain. Fig. 2 shows the IRMPD spectrum of the dehydrated product ion $[AsnAla+H-H_2O]^+$ at *m/z* 186, with the

Table 2
Calculated relative Gibbs free energies in kJ/mol for isomeric structures of the H_2O-loss product from protonated AsnAla for different protonation sites.

Name → ↓ $[H]^+$ Site	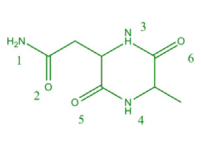 **6 diketopiperazine**	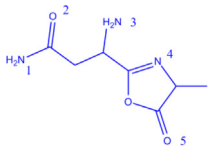 **7 oxazolone**	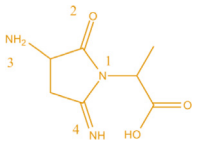 **9 iminopyrrolidinone**
1	+ 72	+ 198	+ 571
2	+ 20	+ 164	+ 146
3	[a]	+ 58	+ 79
4	+ 115	+ 43[b]	+ 13
5	**0**	+ 198	
6	+ 48		

[a] Proton migrates to position 2 during optimization.
[b] Multiple conformers identified; lowest energy is listed.

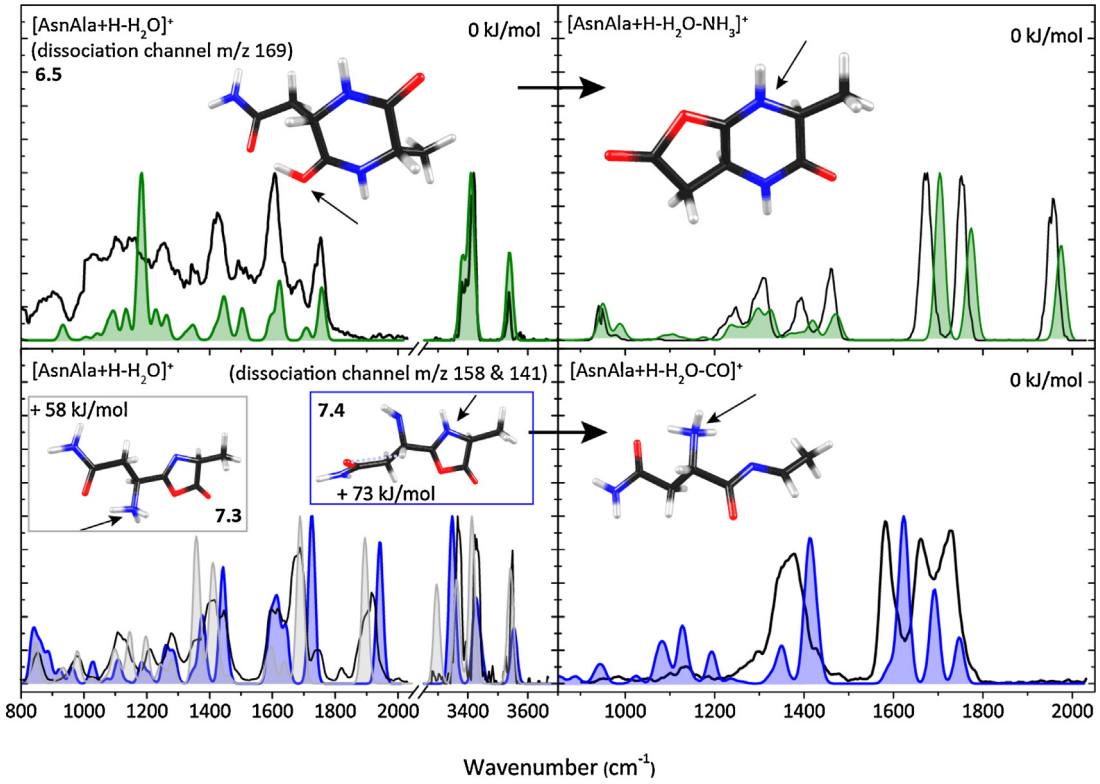

Fig. 2. IRMPD spectra (black) of $[AsnAla+H-H_2O]^+$ (left), $[AsnAla+H-H_2O-NH_3]^+$ (top right) and $[AsnAla+H-H_2O-CO]^+$ (bottom right) compared with the closest matching calculated spectra. The spectrum at the top left is generated from IR dissociation channel *m/z* 169 (sequential loss of NH_3), that at the bottom left is derived from reaction channels *m/z* 158 and 141 (sequential loss of CO and CO+NH_3). Protonation sites are indicated with an arrow.

IR dissociation into channel *m/z* 169 (loss of NH_3) and that into *m/z* 158 + *m/z* 141 (loss of CO and CO + NH_3) again plotted separately.

The spectra encoded into each of these mass channels are substantially different, suggesting again two different *m/z* 186 precursor ion structures to co-exist. The spectrum observed in channel *m/z* 169 (top left in Fig. 2) is attributed to diketopiperazine structure **6**. Note that head-to-tail cyclization of AlaAsn and AsnAla upon H_2O-loss lead to the same structure, so that **6** is in fact equal to **1**. The experimental spectrum matches reasonably well with the spectrum computed for tautomer **6.5**, with the sharp features in 1400–1800 cm^{-1} range reproduced well and the 1000-1400 cm^{-1} range characterized by a series of weaker and unresolved bands. The strong band in the computed spectrum near 1180 cm^{-1} is not observed in the experiment as it is due to a normal mode with substantial O—H^+···O bending character, as discussed above. Our structure assignment is thus the same as that for the $[AlaAsn+H-H_2O]^+$ fragment ion presented in Fig. 1, top left panel. Although the sharp, strong bands in the two experimental spectra coincide closely, discrepancies between the two experimental spectra are also observed. We attribute these discrepancies to the different laser pulse energies used in both experiments, with that for the $[AlaAsn+H-H_2O]^+$ fragment being approximately three times lower, suppressing the weaker bands in the spectrum. The IRMPD spectrum of the MS^3 fragment ion $[AsnAla+H-H_2O-NH_3]^+$ in the top right panel of Fig. 2 suggests that its structure is indeed identical to that established for $[AlaAsn+H-H_2O-NH_3]^+$ and thus provides further support for the structural identification of the MS^2 ion.

The IRMPD spectrum derived from IR induced dissociation channels *m/z* 158 and 141 (Fig. 2, bottom left) possesses a strong and diagnostic feature centered around 1900 cm^{-1}, suggesting an oxazolone structure. As was seen for $[AlaAsn+H-H_2O]^+$ [9,18], this feature is broadened and likely consists of two unresolved bands

due to two oxazolone tautomers, **7.3** and **7.4,** whose calculated spectra are reproduced in grey and blue. For **7.4** (+73 kJ/mol), an alternative conformer substantially lower in energy (+43 kJ/mol) was identified and its computed spectrum is shown in Fig. S2 in the SI. The two spectra differ primarily around 1700 cm^{-1}, but the experimental spectrum does not allow us to assign either one or the other conformer, especially when taking into account the additional contribution from **7.3**, which also has a strong band in this range.

The oxazolone fragment undergoes MS^3 dissociation by sequential CO-loss, as is common for oxazolone *b*-type sequence ions [8]. The spectrum of this MS^3 fragment ion (bottom right in Fig. 2) exhibits bands at 1747 cm^{-1}, C=O stretching of the peptide linkage, 1691 cm^{-1}, C=O stretching of the side chain amide, 1628 cm^{-1}, imine C=N stretching, and 1619 cm^{-1}, NH bending in the NH_3 group. The ion thus has the typical imine structure of *a*-type sequence ions, though with the proton on the N-terminus [54].

Scheme 2b summarizes the suggested reaction mechanism for the loss of H_2O from protonated AsnAla and the sequential losses of NH_3 and CO. Dehydration of protonated AsnAla occurs on the C-terminus and follows bifurcating pathways analogous to those identified for protonated AlaAsn, leading to oxazolone and diketopiperazine isomers. Further activation of the diketopiperazine expels NH_3 from the Asn side chain, forming a 5/6 membered bicyclic structure. In contrast, the oxazolone eliminates CO forming a linear *a*-type sequence ion incorporating an imine group. Inspection of the CID MS^3 spectrum (Fig. S6) suggests relative dissociation rates into the diketopiperazine and oxazolone pathways of 2:1 for dehydration of protonated AsnAla. Although these dissociation pathways are analogous to those of protonated AlaAsn, the relative rates into the two bifurcating pathways are significantly different.

3.3. Dehydrated alanine-glutamine [AlaGln+H-H_2O]$^+$

Six possible reaction pathways for the dehydration of protonated AlaGln are indicated in Scheme 1, leading to five potential structures for the dehydrated ion shown in Tables 3 and S3 in the SI. Nucleophilic attack of the side chain oxygen on the C-terminus and nucleophilic attack of the C-terminal oxygen on the side chain both lead to **13**.

IRMPD of [AlaGln+H-H_2O]$^+$ induces only one fragment at 17 mass units below the precursor ion. Although analogy with the Asn-containing systems above would suggest ammonia-loss to be evidence for a diketopiperazine structure, the IR spectrum recorded is typical for an oxazolone fragment. Fig. 3 shows the experimental IRMPD spectrum (black) compared with calculated IR spectra for the global minimum structure **10.6** (green, top left) and for the oxazolone alternatives **11.3** (dark blue, bottom left) and **11.5** (light grey, bottom left). The band near 1950 cm^{-1} is typical for an oxazolone moiety. A splitting of this band is clearly observed, suggesting the co-existence of two tautomers: **11.3** with protonation on the oxazolone nitrogen and **11.5** with protonation at the N-terminus, the latter being only 6 kJ/mol more stable than the former [9,18]. For **11.3**, the band at 1650 cm^{-1} corresponds to N—H bending at the oxazolone ring and that at 1665 cm^{-1} to N—H bending at the N-terminus. For **11.5**, the bands at 1630 cm^{-1} and 1520 cm^{-1} are assigned to N—H bending vibrations at the N-terminus.

The good match of the experimental spectrum with the oxazolone (**11.3** and **11.5**) spectrum suggests that the diketopiperazine structure (**10.6**) is at best a minor contributor to the population, in contrast with the observations for the Asn analogue. The band at 1755 cm^{-1} in the computed spectrum of **10.6** and the weak band near 1780 cm^{-1} in the observed spectrum that remains unexplained by the oxazolone structures may hint at such a small fraction of diketopiperazine, although both diketopiperazine and oxazolone structures would have to decay by NH_3-loss in this case.

The right panel of Fig. 3 shows the IRMPD spectrum of the MS^3 fragment ion [AlaGln+H-H_2O-NH_3]$^+$ at *m/z* 183. Comparison with theoretical spectra suggests that NH_3 is detached from the oxazolone structure at the N-terminus. The band at 1835 cm^{-1} is due to C=O stretching in the oxazolone ring, that at 1685 cm^{-1} is attributed to C=O stretching in the side chain and the band at 1600 cm^{-1} is due to N—H bending in the side chain.

Scheme 2c summarizes the reaction mechanism. As for the Asn-containing dipeptides, water is lost from the C-terminus, but in this case it leads exclusively to an oxazolone structure. Unlike the oxazolone structures formed from the Asn-containing dipeptides,

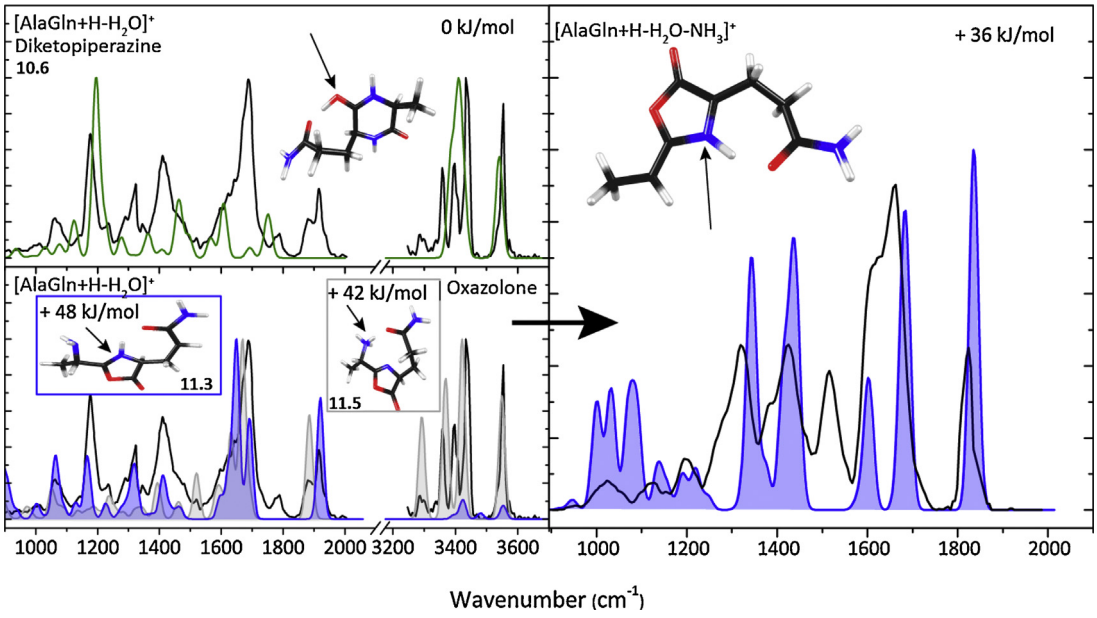

Fig. 3. IRMPD spectrum (black) of [AlaGln+H-H_2O]$^+$ compared against computed spectra for diketopiperazine **10.6** (top left) and oxazolones **11.3** and **11.5** (bottom left). The IRMPD spectrum for the [AlaGln+H-H_2O-NH_3]$^+$ MS^3 fragment ion (right) provides further evidence for an oxazolone structure.

Table 3
Calculated relative Gibbs free energies in kJ/mol for potential ion structures resulting from H_2O loss from protonated AlaGln, each given for different potential protonation sites.

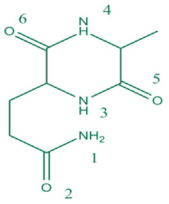
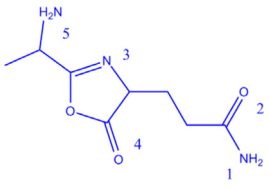
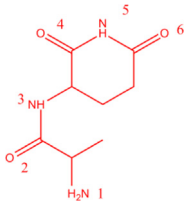

Name → ↓ $[H]^+$ Site	**10 diketopiperazine**	**11 oxazolone**	**12 glutarimide**
1	+ 92	+ 123	+ 13
2	[a]	+ 132	+ 27
3	+ 67	+ 48	+ 119
4	+110	+ 155	[b]
5	+ 35	+ 42	+ 201
6	**0**		+ 146

[a] Proton migrates to position 6 during optimization.
[b] Proton migrates to position 2 during optimization.

Table 4
Calculated relative Gibbs free energies in kJ/mol for possible structures resulting from H_2O loss from protonated GlnAla, each given for different protonation sites.

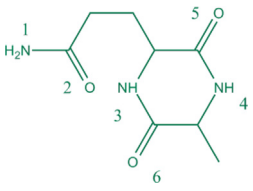

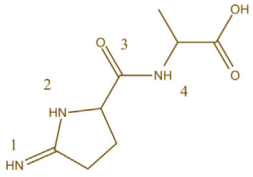

Name → ↓ $[H]^+$ Site	**15 Diketopiperazine**	**16 oxazolone**	**17 imino-proline**
1	+ 86	+ 206	0
2	[a]	[b]	+ 99
3	+ 152	+ 54	+ 146
4	+ 118	+ 91	+ 186
5	+ 83	+ 241	
6	+ 35		

[a] Proton migrates to position 6 during optimization.
[b] Proton migrates to position 3 during optimization.

secondary fragmentation of the oxazolone ion involves the elimination of NH_3 rather than CO.

3.4. *Dehydrated glutamine-alanine, [GlnAla+H-H_2O]$^+$*

Peptides having Glu or Gln as their N-terminal residue are known for their deviating reaction mechanisms [16,55–58]. In particular, NH_3-loss from peptides with an N-terminal Gln residue and H_2O loss from peptides with an N-terminal Glu residue has been shown to form fragments with a pyroglutamyl moiety at the N-terminus [55,57,58]. Nucleophilic attack by the N-terminal nitrogen onto the side-chain δ-carbon atom is in both cases the *modus operandi*. Moreover, it has been previously suggested that doubly-protonated peptide ions that contain glutamine at the N-terminus and a basic or neutral amino acid at the C-terminus eliminate an H_2O molecule from the Gln side chain [55,57,58]. However, the same singly charged peptides were reported to eliminate NH_3 [57,58]. The mechanism proposed for the reaction is a nucleophilic attack of the N-terminal nitrogen on the glutamine side chain leading to the loss of an H_2O molecule [58]. This mechanism follows the brown arrow in Scheme 1 and leads to the formation of structure **17**, which we shall designate by its imino-substituted proline residue. Here we follow the loss of H_2O from singly charged GlnAla.

Table 4 as well as Table S4 in the SI list the five structures resulting from the reaction mechanisms proposed on the bottom row of Scheme 1. Ion **17.1**, the imino-prolinyl structure protonated on the imino nitrogen, is the global minimum. Structures **15** and **16** are the isomeric b_2-type ions resulting from H_2O loss from the C-terminus. Ions **18** and **19** are alternative structures resulting from a nucleophilic attack on the side chain and are not b-type ions.

Fig. 4 compares the experimental spectrum of [GlnAla+H-H_2O]$^+$ with the computed spectrum for imino-prolynyl structure **17.1**. From the favorable agreement between experimental and theoretical spectra particularly in the 1000–2000 cm^{-1} range, we conclude that in contrast to the other dipeptides in this study, protonated GlnAla eliminates H_2O from the Gln side chain and not from the C-terminus. Further support for this assignment comes from the computed spectra for diketopiperazine (**15**) and oxazolone (**16**) structures, which show poor agreement with experiment, see Fig. S4 in the SI. Moreover, the presence of a carboxylic acid group in **17**, but not in **15** and **16**, can explain the observation of H_2O loss as the MS^3 channel, which was not observed for the other dipep-

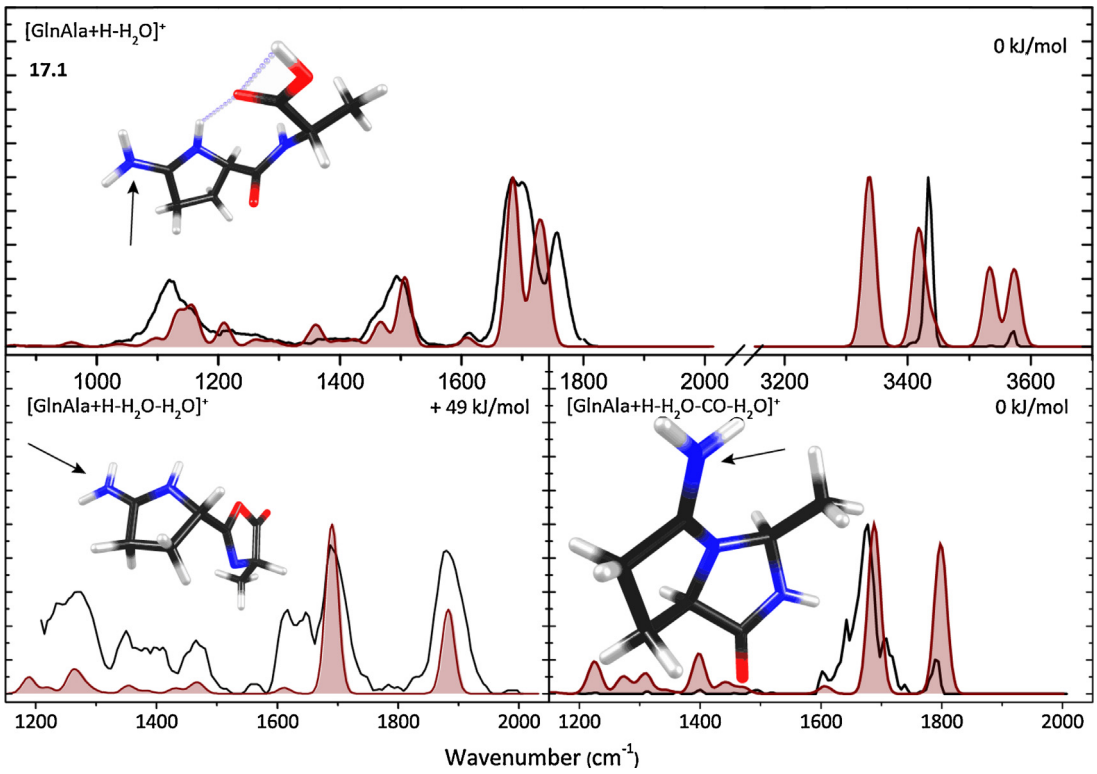

Fig. 4. Experimental IRMPD spectrum of the $[GlnAla+H-H_2O]^+$ MS^2 ion (top) and the $[GlnAla+H-H_2O-H_2O]^+$ MS^3 ion (bottom left) and $[GlnAla+H-H_2O-CO-H_2O]^+$ (bottom right) MS^3 ions, compared against the best matching computed spectra. The relatively poor match between experimental and computed spectra in the H-stretching range for the MS^2 fragment is tentatively attributed to the lower pulse energy of the OPO and/or a relatively high threshold to dissociation for this specific species, which would enhance non-linear effects and prevent excitation to above the threshold on some of the predicted resonances.

tides in this study. As Table 4 indicates, the Gibbs free energies of the oxazolone and diketopiperazine structures are at least 54 and 35 kJ/mol higher than the imino-prolinyl structure, respectively.

In the computed spectrum of **17.1**, the band around 1730 cm^{-1} corresponds to unresolved carboxyl and amide C=O stretches and the band at 1684 cm^{-1} is due to NH_2 bending. The band at 1506 cm^{-1} is due to NH bending of the peptide bond. The spectrum in hydrogen stretching range matches poorly with the computation, but we suspect that this is due to threshold effects, where excitation with the OPO laser is unable to reach up to the dissociation threshold at most frequencies.

Further support for our structural assignment is provided by analysis of the subsequent MS^3 fragments. Secondary CID channels are loss of H_2O and H_2O+CO. The second H_2O is eliminated from the C-terminus leading to the formation of an oxazolone moiety, giving the structure shown in the lower left panel of Fig. 4. The computed IR spectrum for this structure is seen to match fairly well with the experimental spectrum for this MS^3 ion in terms of frequencies, although relative intensities deviate somewhat. The band at 1880 cm^{-1} is due to the oxazolone C=O stretch and the peak at 1697 cm^{-1} is due to the CN stretch of the protonated imine moiety. The predicted spectrum for the $[GlnAla+H-H_2O-CO]^+$ MS^3 ion is also in fair agreement with the experiment in terms of frequencies, although again relative intensities deviate substantially. We suspect that threshold effects in the IRMPD process are at the origin of these deviations. The band at 1800 cm^{-1} is due to the C=O stretch and that at 1690 cm^{-1} to a bending vibration of the amino group.

Scheme 2d presents the suggested reaction mechanism for the dehydration of protonated GlnAla and the suggested pathway for sequential loss of H_2O and CO+H_2O. We conclude that nucleophilic attack occurs from the N-terminus on the glutamine side chain. Dehydration follows the same mechanism as observed for deamidation of the peptide [16,55,58,59]. Moreover, this mechanism is also analogous to deamidation of the Gln amino acid and the dehydration of the Glu amino acid [25]. After dehydration of protonated GlnAla, sequential fragmentation proceeds via two parallel mechanisms, one leading to loss of H_2O from the C-terminus and the other leading to loss of H_2O and CO.

4. Conclusions

Experimental infrared ion spectroscopy combined with quantum-chemical calculations has enabled us to assign the product ion structures resulting from H_2O loss from a series of protonated dipeptides containing Asn or Gln. As well, the structures of several MS^3 fragments were elucidated. From the assigned product ion structures we suggest the reaction mechanisms involved. Combined with our previous study on NH_3 loss from these peptides [16], an extensive molecular structure map of the reaction channels after MS^n can be constructed as shown in Fig. 5.

Our earlier study demonstrated that the deamidation reactions of these dipeptides take place from the Asn or Gln side chain. If we compare the reaction mechanisms assigned for the deamidation reaction with the mechanisms proposed here for the dehydration reaction, we see that only for protonated GlnAla is the mechanism analogous, where the same nucleophilic attack on the side chain takes place during both fragmentation reactions. This is in line with the dehydration reaction of aspartic acid and glutamic acid, where the side chain is attacked by the N-terminus [25]. The assigned structure for protonated GlnAla is not a b_2 ion structure but is in agreement with reported structures [55,57,58]. A diketopiperazine structure has also been found for the b_2 ion of AsnAlaAla [3,9]. For AlaAsnAla the formation of a succinimide structure (which involves the side chain) has been reported [3], but this structure was not

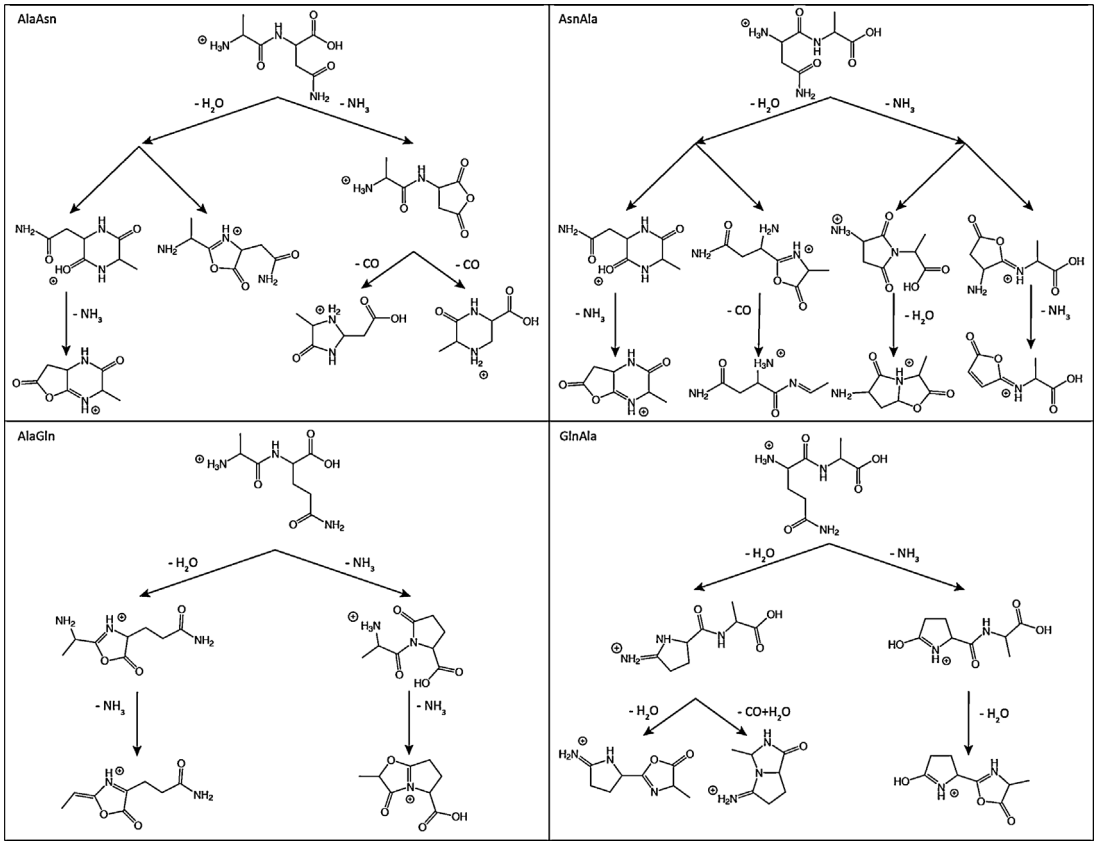

Fig. 5. Molecular structure map of deamidation [16] and dehydration reactions in the Asn and Gln containing protonated dipeptides based on the spectroscopically identified fragment ion structures established.

identified in the dipeptides that contain asparagine in the work presented here. The assigned oxazolone structure for H_2O-loss from protonated AsnAla is in agreement with the oxazolone structure for AsnGly-H_2O previously proposed [38]. However, no bifurcating mechanism to both an oxazolone and diketopiperazine stucture after water loss was proposed [38]. Dehydration of protonated AlaAsn forms the b_2-ion and does not involve the Asn side chain, in contrast to b_2 formation from protonated AlaAsnAla, where the Asn side chain is involved in the formation of a succinimide structure [3]. This suggests that the identity of the third residue is of influence in the formation of b_2-type ions. Detailed transition state calculations are required to explain these observations, where the present structural identification may be used to guide such calculations.

On the basis of the calculated relative Gibbs free energies, the diketopiperazine structures are consistently the lowest energy structures. The observed oxazolone structures have higher relative free energies (48–73 kJ/mol), but are often suggested to form more likely because of kinetic arguments [9,35,60–63,17]. Here, we find that for the Asn-containing peptides, H_2O-loss produces both diketopiperazine and oxazolone structures.

Acknowledgments

The authors gratefully acknowledge the excellent technical support of the FELIX staff. Financial support for this project was provided by NWO Chemical Sciences under VICI project nr. 724.011.002. The authors also thank NWO Physical Sciences (EW) and the SARA Supercomputer Center for providing the computational resources under grant no. 15408 and JO thanks the Stichting Physica. This work is part of the research program of FOM, which is financially supported by NWO.

Appendix A. Supplementary data

Supplementary data associated with this article can be found, in the online version, at **http://dx.doi.org/10.1016/j.ijms.2017.06.004**.

References

[1] W. Li, C. Song, D.J. Bailey, G.C. Tseng, J.J. Coon, V.H. Wysocki, Statistical analysis of electron transfer dissociation pairwise fragmentation patterns, Anal. Chem. 83 (2011) 9540–9545.
[2] J. Grzetic, J. Oomens, Effect of the Asn side chain on the dissociation of deprotonated peptides elucidated by IRMPD spectroscopy, Int. J. Mass Spectrom. 354–355 (2013) 70–77.
[3] J. Grzetic, J. Oomens, Spectroscopic identification of cyclic imide b2-ions from peptides containing Gln and Asn residues, J. Am. Soc. Mass Spectrom. 24 (2013) 1228–1241.
[4] R. Aebersold, D.R. Goodlett, Mass spectrometry in proteomics, Chem. Rev. 101 (2001) 269–296.
[5] H. Steen, M. Mann, The ABC's (and XYZ's) of peptide sequencing, Nat. Rev. 5 (2004) 699–711.
[6] J.R. Yates, Mass spectrometry and the age of the proteome, J. Mass Spectrom. 33 (1998) 1–19.
[7] P. Roepstorff, J. Fohlman, Proposal for a common nomenclature for sequence ions in mass spectra of peptides, Biom. Mass Spectrom. 11 (1984) 601.
[8] B. Paizs, S. Suhai, Fragmentation pathways of protonated peptides, Mass Spec. Rev. 24 (2005) 508–548.
[9] L.J. Morrison, J. Chamot-Rooke, V.H. Wysocki, IR action spectroscopy shows competitive oxazolone and diketopiperazine formation in peptides depends on peptide length and identiy of terminal residue in the departing fragment, Analyst 139 (2014) 2137–2143.
[10] A.R. Dongre, J.L. Jones, A. Somogyi, V.H. Wysocki, Influence of peptide composition gas-phase basicity, and chemical modification on fragmentation efficiency: evidence for the mobile proton model, J. Am. Chem. Soc. 118 (1996) 8365–8374.
[11] V.H. Wysocki, G. Tsaprailis, L.L. Smith, L.A. Breci, Mobile and localized protons: a framework for understanding peptide dissociation, J. Mass Spectrom. 35 (2000) 1399–1406.

[12] R. Boyd, A. Somogyi, The mobile proton hypothesis in fragmentation of protonated peptides: a perspective, J. Am. Soc. Mass Spectrom. 21 (2010) 1275–1278.
[13] R. Spezia, J. Martens, J. Oomens, K. Song, Collision-induced dissociation pathways of protonated Gly2NH2 and Gly3NH2 in the short time-scale limit by chemical dynamics and ion spectroscopy, Int. J. Mass Spectrom. 388 (2015) 40–52.
[14] C.K. Barlow, R.A.J. O'Hair, Gas-phase peptide fragmentation: how understanding the fundamentals provides a springboard to developing new chemistry and novel proteomic tools, J. Mass Spectrom. 43 (2008) 1301–1319.
[15] J.M. Farrugia, R.A.J. O'Hair, G.E. Reid, Do all b2 ions have oxazolone structures? Multistage mass spectrometry and ab initio studies on protonated N-acyl amino acid methyl ester model systems, Int. J. Mass Spectrom. 210–211 (2001) 71–87.
[16] L.J.M. Kempkes, J. Martens, J. Grzetic, G. Berden, J. Oomens, Deamidation reactions of asparagine and glutamine containing dipeptides investigated by ion spectroscopy, J. Am. Soc. Mass Spectrom. 27 (2016) 1855–1869.
[17] N.C. Polfer, J. Oomens, S. Suhai, B. Paizs, Spectroscopic and theoretical evidence for oxazolone ring formation in collision-induced dissociation of peptides, J. Am. Chem. Soc. 127 (2005) 17154–17155.
[18] N.C. Polfer, J. Oomens, S. Suhai, B. Paizs, Infrared Spectroscopy and Theoretical Studies on Gas-Phase Protonated Leu-enkephalin and its fragments: direct experimental evidence for the mobile proton, J. Am. Chem. Soc. 129 (2007) 5887–5897.
[19] G. Frison, G. van der Rest, F. Turecek, T. Besson, J. Lemaire, P. Maître, J. Chamot-Rooke, Structure of electron-capture dissociation fragments from charge-tagged peptides probed by tunable infrared multiple photon dissociation, J. Am. Chem. Soc. 130 (2008) 14916–14917.
[20] S.H. Yoon, J. Chamot-Rooke, B.R. Perkins, A.E. Hilderbrand, J.C. Poutsma, V.H. Wysocki, IRMPD spectroscopy shows that AGG forms an oxazolone b(2)(+) ion, J. Am. Chem. Soc. 130 (2008) 17644–17645.
[21] J. Oomens, S. Young, S. Molesworth, M. van Stipdonk, Spectroscopic evidence for an oxazolone structure of the b2 fragment ion from protonated tri-alanine, J. Am. Soc. Mass Spectrom. 20 (2009) 334–339.
[22] B.J. Bythell, U. Erlekam, B. Paizs, P. Maître, Infrared spectroscopy of fragments from doubly protonated tryptic peptides, Chem. Phys. Chem. 10 (2009) 883–885.
[23] N.C. Polfer, J. Oomens, Reaction products in mass spectrometry elucidated with infrared spectroscopy, Phys. Chem. Chem. Phys. 9 (2007) 3804–3817.
[24] N.C. Polfer, J. Oomens, Vibrational spectroscopy of bare and solvated ionic complexes of biological relevance, Mass Spectrom. Rev. 28 (2009) 468–494.
[25] L.J.M. Kempkes, J.K. Martens, G. Berden, J. Oomens, Deamidation reactions of protonated asparagine and glutamine investigated by ion spectroscopy, Rapid Commun. Mass Spectrom. 30 (2016) 483–490.
[26] B. Lucas, G. Grégoire, J. Lemaire, P. Maître, J. Ortega, A. Rupenyan, B. Reimann, J.P. Schermann, C. Desfrançois, Investigation of the protonation site in the dialanine peptide by infrared multiphoton dissocation spectroscopy, Phys. Chem. Chem. Phys. 6 (2004) 2659–2663.
[27] A.L. Patrick, C.N. Stedwell, B. Schindler, I. Compagon, G. Berden, J. Oomens, N.C. Polfer, Insights into the fragmentation pathways of gas-phase protonated sulfoserine, J. Mass Spectrom. 379 (2015) 26–32.
[28] J. Oomens, J.D. Steill, B. Redlich, Gas-phase IR spectroscopy of deprotonated amino acids, J. Am. Chem. Soc. 131 (2009) 4310–4319.
[29] C.F. Correia, P.O. Balaj, D. Scuderi, P. Maître, G. Ohanessian, Vibrational signatures of protonated: phosphorylated amino acids in the gas phase, J. Am. Chem. Soc. 130 (2008) 3359–3370.
[30] Y.M.E. Fung, T. Besson, J. Lemaire, P. Maître, R.A. Zubarev, Room-temperature infrared spectroscopy combined with mass spectrometry distinghuishes gas-Phase protein isomers, Angew. Chem. 48 (2009) 8340–8342.
[31] U. Erlekam, B.J. Bythell, D. Scuderi, M. van Stipdonk, B. Paizs, P. Maître, Infrared spectroscopy of fragments of protonated peptides: direct evidence for macrocyclic structure of b5 ions, J. Am. Chem. Soc. 131 (2009) 11503–11508.
[32] J.M. Farrugia, T. Taverner, R.A.J. O' Hair, Side-chain involvement in the fragmentation reactions of the protonated methyl esters of histidine and its peptides, Int. J. Mass Spectrom 209 (2001) 99–112.
[33] R.K. Sinha, U. Erlekam, B.J. Bythell, B. Paizs, P. Maître, Diagnosing the protonation site of b2 peptide fragment ions using IRMPD in the X-H (X = O,N and C) stretching region, J. Am. Chem. Soc. Mass Spectrom. 22 (2011) 1645–1650.
[34] G.E. Reid, R.J. Simpson, R.A.J. O'Hair, A mass spectrometric ab initio study of the pathways for dehydration of simple glycine and cysteine-containing peptide [M+H]+ ions, J. Am. Soc. Mass Spectrom. 9 (1998) 945–956.
[35] B. Balta, V. Aviyente, C. Lifshitz, Elimination of water from the carboxyl group of GlyGlyH+, J. Am. Chem. Soc. 14 (2003) 1192–1203.
[36] K.D. Ballard, S.J. Gaskell, Dehydration of peptide [M +H]+ ions in the gas phase, J. Am. Soc. Mass Spectrom. 4 (1993) 477–481.
[37] S. Zou, J. Oomens, N.C. Polfer, Competition between diketopiperazine and oxazolone formation in water loss products from protonated ArgGly and GlyArg, Int. J. Mass Spectrom. 316–318 (2012) 12–17.
[38] G.C. Boles, R.R. Wu, M.T. Rodgers, P.B. Armentrout, Thermodynamics and mechanisms of protonated asparaginyl-glycine decomposition, J. Phys. Chem. B. 120 (2016) 6525–6545.
[39] B.R. Perkins, J. Chamot-Rooke, S.H. Yoon, A.C. Gucinski, A. Somogyi, V.H. Wysocki, Evidence of dikeopiperazine and oxazolone structures for HA b2+ ion, J. Am. Chem. Soc. 131 (2009) 17528–17529.
[40] U.H. Verkerk, J. Zhao, M.J. van Stipdonk, B.J. Bythell, J. Oomens, A.C. Hopkinson, K.W.M. Siu, Structure of the [M+H-H2O]+ ion from tetraglycine: a revisit by means of density functional theory and isotope labeling, J. Phys. Chem. A 115 (2011) 6683–6687.
[41] J. Martens, J. Grzetic, G. Berden, J. Oomens, Structural identification of electron transfer dissociation products in mass spectrometry using infrared ion spectroscopy, Nat. Commun. 7 (2016) 11754–11760.
[42] J. Martens, G. Berden, C.R. Gebhardt, J. Oomens, Infrared ion spectroscopy in a modified quadrupole ion trap mass spectrometer at the FELIX free electron laser laboratory, Rev. Sci. Instrum. 87 (2016) 103108–103115.
[43] D. Oepts, A.F.G.v.d. Meer, P.W.v. Amersfoort, The free-electron-laser user facility FELIX, Infrared Phys. Technol. 36 (1995) 297–308.
[44] J.K. Martens, J. Grzetic, G. Berden, J. Oomens, Gas-phase conformations of small polyprolines and their fragment ions by IRMPD spectroscopy, Int. J. Mass Spectrom 377 (2015) 179–187.
[45] J. Oomens, B.G. Sartakov, G. Meijer, G. von Helden, Gas-phase infrared multiple photon dissociation spectroscopy of mass-selected molecular ions, Int. J. Mass Spectrom. 254 (2006) 1–19.
[46] M.J. Frisch, G.W. Trucks, H.B. Schlegel, G.E. Scuseria, M.A. Robb, J.R. Cheeseman, G. Scalmani, V. Barone, B. Mennucci, G.A. Petersson, H. Nakatsuji, M. Caricato, X. Li, H.P. Hratchian, A.F. Izmaylov, J. Bloino, G. Zheng, J.L. Sonnenberg, M. Hada, M. Ehara, K. Toyota, R., Fukuda, J. Hasegawa, M. Ishida, T. Nakajima, Y. Honda, O. Kitao, H. Nakai, T. Vreven, J. Montgomery, J.A., J.E. Peralta, F. Ogliaro, M. Bearpark, J.J. Heyd, E. Brothers, K.N. Kudin, V.N. Staroverov, R. Kobayashi, J. Normand, K. Raghavachari, A. Rendell, J.C. Burant, S.S. Iyengar, J. Tomasi, M. Cossi, N. Rega, N.J. Millam, M. Klene, J.E. Knox, J.B. Cross, V. Bakken, C. Adamo, J. Jaramillo, R. Gomperts, R.E. Stratmann, O. Yazyev, A.J. Austin, R. Cammi, C. Pomelli, J.W. Ochterski, R.L. Martin, K. Morokuma, V.G. Zakrzewski, G.A. Voth, P. Salvador, J.J. Dannenberg, S. Dapprich, A.D. Daniels, O. Farkas, J.B. Foresman, J.V. Ortiz, J. Cioslowski, D.J. Fox, Gaussian09, RevisionA.1. *Gaussian, Inc Wallingford, CT* (2009).
[47] D.A. Case, T. Darden, T.E. Cheatham III, C. Simmerling, J. Wang, R.E. Duke, R. Luo, R.C. Walker, W. Zhang, K.M. Merz, B.P. Roberts, S. Hayik, A. Roitberg, G. Seabra, J. Swails, A.W. Goetz, I. Kolossváry, K.F. Wong, F. Paesani, J. Vanicek, R.M. Wolf, J. Liu, X. Wu, S.R. Brozell, T. Steinbrecher, H. Gohlke, Q.X. Cai Ye, J. Wang, M.-J. Hsieh, G. Cui, D.R. Roe, D.H. Mathews, M.G. Seetin, R. Salomon-Ferrer, C. Sagui, V. Babin, T. Luchko, S. Gusarov, A. Kovalenko, P.A. Kollman, AMBER, University of California, San Francisco, 2012.
[48] J.M. Headrick, E.G. Diken, R.S. Walters, N.I. Hammer, C.R.A, J. Cui, E.M. Myshakin, M.A. Duncan, M.A. Johnson, K.D. Jordan, Spectral signatures of hydrated proton vibrations in water clusters, Science 308 (2005) 1765–1769.
[49] P. Hurtado, F. Gamez, H.S, B. Martinez-Haya, J.D. Steill, J. Oomens, Crown ether complexes with H3O+ and NH4+: proton localization and proton bridge formation, J. Phys. Chem. A 115 (2011) 7275–7282.
[50] X. Li, J. Oomens, J.R. Eyler, D.T. Moore, S.S. Iyengar, Isotope dependent, temperature regulated, energy repartitioning in a low-barrier, short-strong hydrogen bonded cluster, J. Chem. Phys. 132 (2010) 244301–244315.
[51] J.M. Headrick, J.C. Bopp, M.A. Johnson, Predissociation spectroscopy of the argon-solvated H5O2+ "zundel" cation in the 1000–1900 cm-1 region, J. Chem. Phys. 121 (2004) 11523–11526.
[52] T.D. Fridgen, L. MacAleese, P. Maitre, T.B. McMahon, P. Boissel, J. Lemaire, Infrared spectra of homogeneous and heterogeneous proton-bound dimers in the gas phase, Phys. Chem. Chem. Phys. 7 (2005) 2747–2755.
[53] T.D. Fridgen, T.B. McMahon, L. MacAleese, J. Lemaire, P. Maitre, Infrared spectrum of the protonated water dimer in the gas phase, J. Phys. Chem. A 108 (2004) 9008–9010.
[54] V.H. Wysocki, K.A. Resing, Q. Zhang, G. Cheng, Mass spectrometry of peptides and proteins, Methods 35 (2005) 211–222.
[55] B. Godugu, P. Neta, Y. Simon-Manso, S.E. Stein, Effect of N-terminal glutamic acid and glutamine on fragmentation of peptide ions, J. Am. Soc. Mass Spectrom. 21 (2010) 1169–1176.
[56] N.N. Dookeran, T. Yalcin, A.G. Harrison, Fragmentation reactions of protonated alpha-amino acids, J. Mass Spectrom. 31 (1996) 500–508.
[57] A.G. Harrison, Fragmentation reactions of protonated peptides containing glutamine or glutamic acid, J. Mass Spectrom. 38 (2003) 174–187.
[58] P. Neta, Q. Pu, L. Kilpatrick, X. Yang, S.E. Stein, Dehydration versus deamination of N-terminal glutamine in collision-induced dissociation of protonated peptides, J. Am. Soc. Mass Spectrom. 18 (2007) 27–36.
[59] M.A. Baldwin, A.M. Falick, B.W. Gibson, S.B. Prusiner, N. Stahl, A.L. Burlingame, Tandem mass spectrometry of peptides with N-terminal glutamine: studies on a prion protein peptide, J. Am. Soc. Mass Spectrom. 1 (1990) 258–264.
[60] P.B. Armentrout, A.L. Heaton, Thermodynamics and mechanisms of protonated diglycine decomposition: a computational study, J. Am. Chem. Soc. 23 (2012) 621–632.
[61] T. Yalcin, I.G. Csizmadia, M.R. Peterson, A.G. Harrison, The structure and fragmentation of bn ($n \geq 3$) ions in peptide spectra, J. Am. Soc. Mass Spectrom. 7 (1996) 233–242.
[62] M.J. Nold, C. Wesdemiotis, T. Yalcin, A.G. Harrison, Amide bond dissociation in protonated peptides. Structures of the N-terminal ionic and neutral fragments, Int. J. Mass Spectrom. Ion Processes 164 (1997) 137–153.
[63] B. Paizs, S. Suhai, Combined quantum chemical and RRKM modeling of the main fragmentation pathways of protonated GGG II. Formation of b2, y1, and y2 ions, Rapid Commun. Mass Spectrom. 16 (2002) 375–389.